The Thesis Committee for Rahul Milind Moghe
certifies that this is the approved version of the following thesis:

Muscle activation patterns for voluntary isometric stiffness in human index finger

APPROVED BY

SUPERVISING COMMITTEE:

Ashish D. Deshpande, Supervisor

James Sulzer

Muscle activation patterns for voluntary isometric stiffness in human index finger

by

Rahul Milind Moghe, B.Tech.

THESIS

Presented to the Faculty of the Graduate School of

The University of Texas at Austin

in Partial Fulfillment

of the Requirements

for the Degree of

MASTER OF SCIENCE OF ENGINEERING

THE UNIVERSITY OF TEXAS AT AUSTIN

May 2017

Dedicated to my parents

Acknowledgments

First, I wish to thank my lab mates who helped and supported me throughout my stay at UT Austin. They were the reason this work was possible and they made it enjoyable for me. I would like to thank my advisor Prof. Ashish D. Deshpande for giving me the freedom to do what I want supporting and pushing me. Lastly, I would like to thank Dr. Youngjin Na, Prof. James Sulzer and Alfredo Serrato, without them, this thesis could not have been completed.

Muscle activation patterns for voluntary isometric stiffness in human index finger

Rahul Milind Moghe, M.S.E.
The University of Texas at Austin, 2017

Supervisor: Ashish D. Deshpande

Humans can voluntarily control their finger stiffness for grasping and manipulation tasks. A long standing question in biomechanics is aimed at understanding the criterion used by the cenrtal nervous system to control the motor output of human limbs. Humans are known to voluntarily control their limb posture, end-tip force and stiffness. This thesis concerns itself with controlling stiffness in isometric conditions only. This work examines the variability of voluntary isometric stiffness modulation for the index finger at constant fingertip force. Previous studies either investigated muscle synergies responsible for different force-stiffness conditions or only measured behavioral measures of stiffness. However, the variability of stiffness for constant force condition was not explained. In this study, the stiffness of the index finger was modulated while maintaining a constant isometric fingertip force at 4 different force magnitudes and 2 different force directions. The muscle activations

of 7 muscles that are related to the index finger were measured using surface electromyography (sEMG) sensors. Synergies estimated from a principal component analysis (PCA) using the recorded sEMG showed that the contribution of one synergy explains 80-95% of the variation in the data. The degree of alignment was used to analyze these stiffness synergies for different force conditions. The minimum mean value of degree of alignment was found for the comparison between synergies at high forces. However, comparison of synergies at lower forces showed that the stiffness synergy varies more with the forcing direction than it does with force magnitude. These results show the existence of a stiffness synergy to modulate the stiffness for individual force direction regardless of the magnitude of force level. Although the results at higher forces do not agree with this conclusion, stiffness modulation is prominent only at lower forces. This result gives an insight into what muscle synergies are important for modulating the fingertip stiffness. It can prove useful in robotics applications to simplify stiffness modulation without explicitly calculating inverse kinematics and also in restoring stiffness modulation after hand injury.

Table of Contents

List of Tables

List of Figures

Chapter 1

Introduction

1.1 Problem Description

Determining redundant motor control strategies has been a long standing question in biomechanics. This question is about the strategies that the central nervous system (CNS) adopt to control the motor output of human limbs. In any grasping and manipulation tasks, humans are known to voluntarily control 3 fundamental outputs of their limbs, i.e., the pose, the endtip force and stiffness of each of their digits. Due to a redundant musculature of human limbs [6], there exist theoretically infinite ways of activating the muscles to achieve the same fingertip force. Inspite of this redundancy, the CNS has been known to use repeatable and systematic neuromuscular strategies to achieve a given task. Understanding these neuromuscular strategies will greatly aid in rehabilitation and prosthetic applications, where the focus is on restoring and repairing our ability to voluntarily generate the 3 fundamental outputs. It can also prove useful in robotic applications where these new control strategies can be tested and compared with the conventional ones.

Many studies have been conducted to understand the relation between muscle lengths and finger pose [52], [21], [7], [8], [12], [3]. These studies also

delineate the relation between joint torques and muscle forces. A lot of work was aimed towards understanding what muscle forces are required to generate endtip force [34], [49], [44], [48]. Researchers have worked extensively on muscle activation optimization criterion for finding the muscle activation patterns for achieving a given fingertip force [36], [17]. However, these studies did not account for the voluntary co-contraction in human fingers which produced different finger stiffness for the same fingertip force. As a result, these methods failed to provide accurate estimates of muscle forces in all cases. Certain EMG-constrained optimization methods were used to estimate the co-contraction while solving for muscle activation patterns [2], [51], [22], [13]. Hence, understanding the problem of modulating finger stiffness by varying muscle forces was essential. This thesis focuses on the index finger, a limb central to all manipulation tasks performed by humans.

Previous studies on voluntary stiffness control have examined behavioral stiffness measures of the limb, i.e., the shape, orientation and volume of the fingertip stiffness ellipsoid. [35] showed that the 2 dimensional stiffness ellipse orientation for the arm can not be changed to a large degree by humans during force regulation tasks. They concluded that it was unlikely that the stiffness orientation was controlled independent of the end-tip force. [31] studied the voluntary stiffness control for the index finger. They showed that the 2 dimensional stiffness ellipse orientation was roughly parallel to the proximal phalanx and hardly affected by the finger posture and direction of fingertip force. [1] studied the dependence of endtip force magnitude and direction on

stiffness ellipsoid. Although, it is theoretically possible to control all three of them, it was shown that humans can effectively only change the volume or the magnitude of stiffness. This is an important result which is used in this study. This thesis, however, investigates the physiological measures for stiffness control, meaning, the muscle activation patterns required to change the index fingertip stiffness. Fewer studies have measured the muscle activations for stiffness control. The experiments conducted in [4] showed that two different muscle synergies exist for the voluntarily controlling 4 force-stiffness conditions. However, they did not look at the muscle synergy responsible for the change in synergy, rather they only analysed the muscle synergy at different force-stiffness conditions. Also, the muscle synergy was normalized by the sum of the muscle activations and hence did not distinguish between different levels of stiffness.

In this work, the stiffness variations on different iso-torque manifolds for the index finger are analysed. Essentially, the muscle synergies responsible for stiffness modulation are measured keeping the pose and the fingertip force constant. Since, this is difficult task for humans to achieve, a unique experimental platform is explained in this work to simplify this task for the humans. Using this setup, the requirement of maintaining force and pose is reduced to a requirement of maintaining pose only. This simplifies the task for the human subject study and much more accurate data can be obtained. The experiments conducted are tested against the hypothesis that although different muscle synergies are available to humans to achieve the given stiffness, humans

used a simplified approach to controlling stiffness. It is hypothesized that the CNS uses a single muscle synergy to control the index finger stiffness. In order to achieve a given force-stiffness condition, 2 muscle synergies required, one for the force and the second one to change the stiffness. This hypothesis talks about the second synergy required to change the stiffness while maintaining a constant fingertip force. The subjects participating in the experiments are asked to maintain a constant finger pose while co-contracting their muscle to stiffen their index finger. Continuous surface EMG, force and RGB data are collected during the tests to test the hypothesis and validate the assumptions.

1.2 Thesis Overview

This thesis makes the following contributions:

- A unique experimental platform required to maintain a constant pose and endtip force. This platform can be used by other researchers to test isometric force-stiffness conditions generated by human limbs. This can also be modified further to measure the endtip stiffness without using n-link robots.
- An important result about isometric stiffness modulation of human index finger which gives some insight into the neuromuscular strategies used by the CNS for stiffness control.
- Some opinions about neuromuscular strategies that the index finger

might be following based on the results obtained through the experiments explained in this thesis.

It is important to know that this thesis does not find a mapping between the muscle activations and the fingertip stiffness. This thesis investigates the strategies for stiffness changes rather than achieving specific stiffness values. The roadmap for this thesis is as follows. Chapter 2 is a literature review of the previous studies in this field. This chapter also explains the musculoskeletal model of the index finger and some mathematical preliminaries like the iso-torque framework [1] which are useful for understanding this thesis. This thesis uses a systemic approach to modeling the index finger. It also reviews the literature for stiffness control and neuromuscular strategies used for redundancy resolution. It states some examples of optimization models for force distribution and states certain hypothesis for neuromuscular control in the past.

Chapter 3 describes the methods used in the experiments. The experimental setup is described in detail along with the data acquisition hardware and software used. It also lists down the protocol used during the experiments including the instructions given to the subjects during the experiment. The rest of the thesis, chapter 4 lists the results and observations obtained during the experiments and chapter 5 gives the interpretation of results in view of the hypothesis and lists new avenues of research that can be explored with this thesis.

Chapter 2

Background

This chapter is a literature review of the previous work in related fields and also lists down the mathematical preliminaries needed to understand the thesis. It also states the musculoskeletal model of the index finger used in this thesis. The iso-torque manifold is derived for the index finger. Previous contributions in index finger stiffness are listed and the differences between them and this work are established. Other work between endpoint stiffness is also acknowledged. Finally, the significance of this work to the muscle redundancy problem is explained and how it synergizes with certain optimization models and other theories is explained.

2.1 Biomechanical Model

The index finger has 4 degrees of freedom, namely, DIP flexion-extension, PIP flexion-extension, MCP flexion-extension and MCP ad-abduction. Index finger is known to be controlled by 7 independent muscles. They are first lumbrical (LUM), first dorsal interosseous (DI), first palmar interosseous (PI), extensor indicis (EI), extensor digitorum (ED), flexor digitorum superficialis (FDS) and flexor digitorum profundus (FDP). The first 3 are called intrinsic

Muscle Name	Max muscle force (N)
LUM	5
DI	37
PI	31
EI	24
ED	24
FDS	48
FDP	65

Figure 2.1: The maximum muscle forces that can be produced [33].

muscles as they are intrinsic to the human hand while the others are called extrinsic. The extrinsic muscles are much stronger than the intrinsic muscles. The table 2.1 shows the maximum force that every muscle can produce. It can be seen that the flexors are much more powerful as compared to the other muscles. Fig 2.2 show the anatomical structure of the index finger showing its muscles.

2.2 Force and stiffness

The moment arm matrix R is the matrix that explains the relation between the joint torques and muscle forces. The Jacobian matrix J is the matrix denoting the relation between the joint torques and fingertip force. In this thesis, only the isometric force and stiffness production of the index finger is considered. This means that both the moment arm matrix and the Jacobian matrix are considered to be constant. For a constant finger pose, the relation between muscle activation and muscle forces is considered to be linear [23].

$$f_m = F_{max}\ a_m \tag{2.1}$$

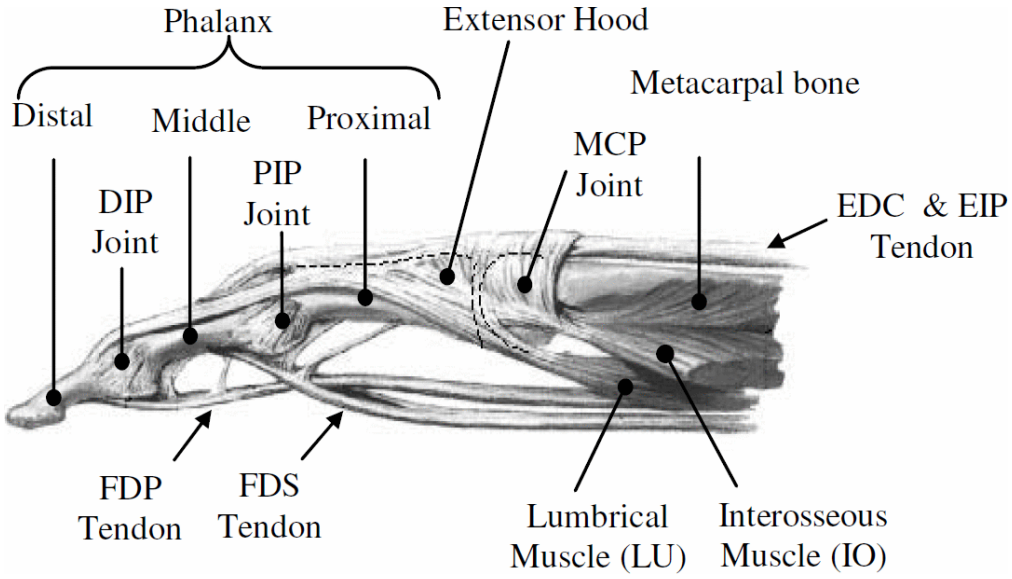

Figure 2.2: Tendon structure of the index finger [10]

Here, $f_m \in \mathbb{R}^7$ vector of muscle forces, $F_{max} \in \mathbb{R}^{7\times7}$, while $a_m \in \mathbb{R}^7$ is a vector of muscle activations. Using kinematics relations, the fingertip force is given as follows:

$$f_{end} = J^{-T} R F_{max}\ a_m \tag{2.2}$$

The fingertip stiffness is given by differentiating the force with respect to fingertip position. It can be written with respect to the muscle stiffness vector k_m as follows:

$$k_{end} = J^{-T} R k_m R^T J^{-1} \tag{2.3}$$

This thesis does not use the exact value of the stiffness. The muscle stiffness used in earlier studies has been assumed to have linear or exponential relation to muscle force [24], [9], [14] [39].

2.3 Iso-Torque Manifold

[1] laid down the framework for the iso-effector space for the index finger. In this thesis, the iso-torque manifold is used from the framework to understand the isometric stiffness modulations for the index finger. The iso-torque manifold is the space of all muscle forces responsible for generating the same fingertip force in isometric conditions. Assuming linear activation to muscle force relationship Eq 2.1, the iso-torque manifold is a 3 dimensional hyperplane in a 7 dimensional muscle activation space as a result of 4 constraints from Eq 2.2. Hence, isometric stiffness modulations live in this iso-torque hyperplane which is 3 dimensional.

2.3.1 Voluntary Stiffness Control

The muscle redundancy problem has been studied for decades by researchers to understand how the central nervous system (CNS) control the human body. As for hands, investigating the neuromuscular control by CNS have shown promising results in the field of force control of human hands [44], [48]. Researchers have come up with many theories to explain the distribution of muscle forces for a given fingertip forces, like optimal control of muscle forces and uncontrolled manifold hypothesis (UCM). However, the field of stiffness control of human fingers has recieved attention only recently as the optimization models were unable to explain the co-contraction in index fingers. The CNS is known to control the motor output of the individual finger, which consists of, the finger pose, fingertip force and fingertip stiffness. This thesis aims

to examine the third motor output, i.e., the stiffness.

Although humans are known to control the entire stiffness ellipsoid voluntarily, this work assumes that humans can not control all the 3 parameters independently. Humans can only co-contract the index finger by changing one parameter equivalently represented as the stiffness of the index finger. The work by [1], [35], [31] leads to hypothesize that the CNS uses simplified strategies for controlling the stiffness of the index finger in isometric conditions. The inability of humans to change the stiffness ellipse orientation to a great degree motivates this hypothesis.

Chapter 3

Methods

3.1 Introduction

In the chapter 2, the redundant musculature of the index finger was discussed using the null space of the moment arm matrix. The iso-troque spaces formed as a result of the null space are an intuitive way of understanding muscle synergies. The goal is to understand which muscle synergies are responsible for stiffness changes in the index finger. One way of doing this is to fix the index finger pose and endtip force and look at the muscle activation by varying the stiffness. In order to achieve this, an experimental platform was developed for a study. This chapter explains the setup and the protocol in detail along with the criterion for subjects.

3.2 Experimental Setup

This section describes the experimental platform used for healthy human subject study. This setup was based on the concept that fixing the elongation of a spring results in a constant force applied externally by the spring. Hence, if the fingertip was able to maintain constant elongation of the spring, the finger pose and fingertip force are inherently fixed. As shown in Fig. 3.3,

3D printed cuffs were made to rest the forearm and the wrist on the ulnar side of the right hand. Velcros on these cuffs were used to prevent movement of the wrist and the forearm. An ATI 6-axis force sensor was fixed onto a platform which slides on bearings. The bearings were fixed to the base. The platform was connected to a spring which was further connected to the circumference of a wheel through a string. The wheel was rigidly fixed to the shaft of a geared high torque DC Motor (0.5 RPM, 137 kg/m stall torque). The front part of the force sensor was covered with a 3D printed plate. The plate had a protruding circular part for the index finger to apply forces on. The position of the cuffs relative to the sliding platform was customized for every subject so that, in the relaxes position, the index fingertip touched the center of the protruding part. This relaxed position of the index finger approximately corresponded to 10° DIP flexion, 45° PIP flexion, 45° MCP flexion and 0° MCP ad-abduction. Another 3D printed holder was made to hold the force sensor on the platform in the center position while the natural position of the spring was being changed using the motor. 5 $\frac{1}{4}$" red dot markers were placed on the index finger and RGB data was collected during the trials to validate the finger pose. The subjects were asked to refrain from moving their index finger after the commencement of each set of trials.

3.3 Subjects

14 right-handed individuals (10 males, 4 females; age 24.9 ± 3.6 yr; mean ± SD) that participated had no history of hand injury or dysfunction.

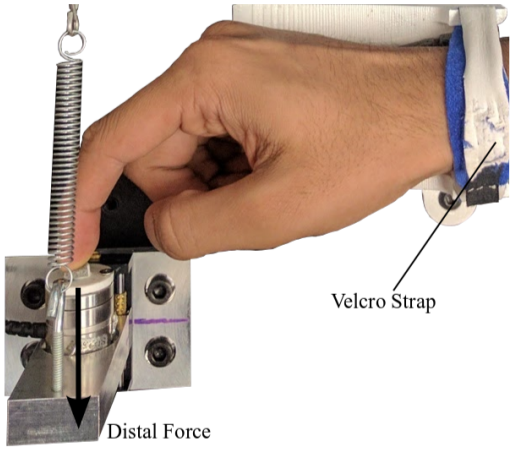

Figure 3.1: Setup for distal forcing condition.

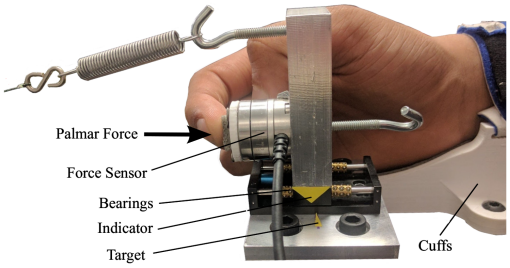

Figure 3.2: Setup for palmar forcing condition.

Figure 3.3: This figure shows the experimental setup for palmar forces. An indicator and target is provided for the subjects to match their.

The study protocol and consent form were approved by the Institutional Review Board and all participants were provided informed, written consent prior to study participation.

3.4 Electromyography

7 surface EMG sensors (Delsys, Boston, MA) were used to collect data from index finger muscles. The muscles of the forefinger are first lumbrical (LUM), first dorsal interosseous (DI), first palmar interosseous (PI), extensor indicis (EI), extensor digitorum (ED), flexor digitorum superficialis (FDS) and flexor digitorum profundus (FDP). The sEMG placements were similar to the ones used for fine-wire EMGs explained in [11] . The position of the sensors were adjusted based on the data from the sensors before comitting to the EMG placements. Before starting the trials, the EMG data from each of the sensors was streamed using NI LabVIEW software and the positions were verified using palpation. The data collected from the sEMG sensors was a 7 dimensional muscle activation vector.

$$\vec{a} = \left[a_{LUM}, a_{DI}, a_{PI}, a_{EI}, a_{ED}, a_{FDS}, a_{FDP}\right]^T \tag{3.1}$$

3.5 Vision Data Markers

5 red dot markers were placed on the index finger, 3 on the joints and 2 for reference. RGB data was collected from a camera placed directly above the index finger. This data was collected only for the stiffness tests and not

for the Offset and MVC tests.

3.6 Experiment Protocol

The length of the 3 phalanges were measured using a digital caliper before the start of the experiment. This experiment was divided into 2 sets of trials based on whether the forces applied by the index finger are in the distal or palmar direction. These two directions were chosen because the other 3 directions are rarely used for force production. In each set, the subjects were asked to perform 3 types of tests:

- The offset test
- Maximum Voluntary Contraction Test
- 4 stiffness modulation tests

A flow chart for experiment protocol is shown in Fig 3.4. The numbers next to the trials are used as a shorthand notation, e.g., d60 - distal 60% MVF stiffness trial, etc. Also, S_{d60}:S_{p40} will be used to denote comparison of principal synergies between distal 60% and palmar 40% trials for particular force direction.

3.6.0.1 Offset Test

In this test the subjects were asked to relax their index finger for 2 seconds while continuous data from the sEMG and the force sensor was collected.

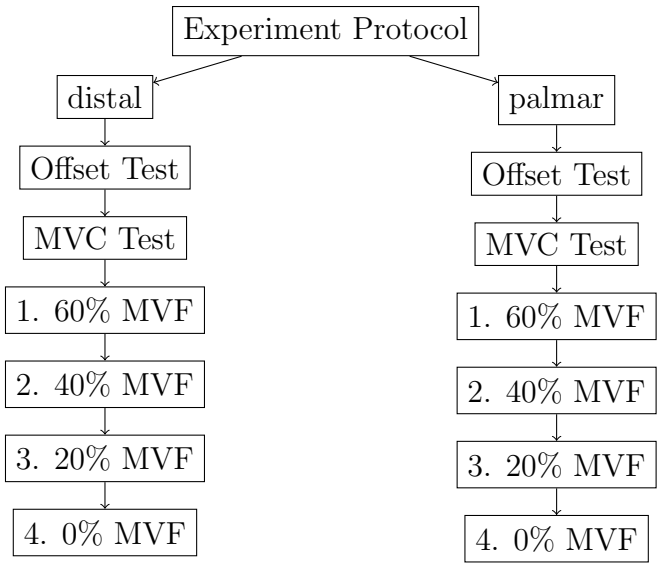

Figure 3.4: Experiment Protocol.

The finger was not in contact with the force sensor for this test and no spring was used and vision data was not collected.

3.6.0.2 MVC Test

In this test, a metal block of suitable dimension was placed behind the sliding platform to hold the platform in the center position. The subjects were asked to push the force sensor on the sliding platform with maximum possible force 3 times. They were asked to complete all the 3 MVCs in 15 seconds. They were asked to use only the index finger to achieve maximum force. sEMG and force data were collected for this test and filtered force data was shown on the screen as bio-feedback to the subjects while they were doing this test. Subjects were motivated verbally to do better.

3.6.0.3 Stiffness Test

The maximum force obtained from the MVC test was then used to calculate 20%, 40% and 60% of their maximum voluntary force (MVF). This test consists of 4 trials corresponding to the force magnitude of 60%, 40%, 20% and 0% MVF. The platform holder described above was put in place to hold the sliding platform. A spring suitable to the force magnitude was chosen and connected in series, between the platform and the DC motor. The extension of the spring was manually set using the DC motor so that the force with which it pulls when the sliding platform is in the center position is equal to the force magnitude for that trial. Although the same spring could have been used for all the force magnitudes, the springs with smaller stiffness were preferred in each trial to make the fingertip force robust to pose perturbations.

Once the force was set, the holder was removed and the subjects were asked to hold the platform in the center position and co-contract or stiffen and relax their index finger 3 times all while maintaining their finger pose and hence, their fingertip force. Since, this was a difficult task, the subjects were given ample practice before the experiments to get them accustomed to these stiffness modulation tests. The data collected for these trials were vision data of their finger, force data and sEMG data. The sum of all the muscle activations was displayed on the screen to see whether the subjects were co-contracting their muscles. This is similar to the index of muscle co-contraction around the joint (IMCJ) from . There was no time limit for this test and verbal cues to stiffen and relax their fingers were provided during the experiment.

3.7 Data Collection

Two NI DAQ Modules (NI USB 6321 and NI 6356 PCIe) and LabVIEW software (National Instruments, Inc., Austin, TX) were used to program the stiffness protocol and collect sEMG and force data. A 16-channel Delsys Trigno Wireless EMG system with Trigno Mini sensors (Delsys Inc., Boston, MA) was used to collect sEMG data. An ATI 6-axis force sensor (Nano25) was used to collect force data during the isometric contractions. The analog output signals from the sEMG system were connected to the analog input channels of the NI USB 6321 module. The analog output signal from the force sensor was connected to the NI 6356 module, which is a DAQ card in the desktop. The LabVIEW software architecture consisted of three VIs, one for reading and setting the force sensor values, one for testing the sEMG data before commiting to a position of sEMG sensor and one for performing the offset, MVC and stiffness trials. Using this software, the sEMG and force data were collected concurrently at just below 2000 Hz. Raw data was exported for additional processing and analyzed using MATLAB (The Mathworks, Natick, MA). Video was recorded for the stiffness trial in all experiments using 12.3 MP camera at the rate of 30 frames per second.

3.8 Data Processing

This section describes the data processing techniques used on the collected data before inferring conclusions on them.

3.8.1 EMG Data Processing

The set of sEMG data for each subject consists of 2 sets of data for the fingertip forcing in the palmar and the distal direction respectively. Each set of data consists of offset data, maximum voluntary contraction (MVC) data and data from 4 trials each for 60%, 40%, 20% and 0% maximum voluntary force (MVF).

3.8.1.1 Offset Data

A straightforward average of the data collected for 2 seconds was taken to get the offset values for each of the 7 muscles.

3.8.1.2 MVC Data

The MVC data, which was collected for 15 seconds was processed as follows:

- The calculated offsets were subtracted from the data for each muscle
- Data was band pass filtered from 20 Hz to 450 Hz
- Data was full-wave rectified
- Maximal value was calculated
- Perform same process on the data from the trials and find the maximum activation value for each muscle during trials

- Compare the MVC value from the MVC test and the stiffness trials and get the maximum MVC for each muscle

3.8.1.3 Stiffness Data

The data from the stiffness trials were processed as follows [15], [30]:

- The calculated offsets were subtracted from the data for each muscle
- Data was band pass filtered from 20 Hz to 450 Hz
- Data was full-wave rectified
- Muscle data was divided by their respective MVC values
- Data was down-sampled with a moving average filter with a window 500 samples
- A principal component analysis (PCA) was performed on the entire data from each of the 4 trials

3.8.2 Force Data Processing

Each set of data corresponding to the fingertip force direction consists of 4 force data sets corresponding to 60%, 40%, 20% and 0% maximum voluntary fingertip force ($F_x,\ F_y,\ F_z$). Each force data was processed as follows:

- Offset values were calculated as average of the 0% MVf case and subtracted from all the data sets of that case (distal or palmar)

- Low pass filtered with the cut-off frequency at 4 Hz
- 1200 data points were rejected from the beginning of the trial
- The mean and the standard deviation of the data was calculated

3.8.3 Vision Data Processing

Vision data was collected for every trial except for the offset and mvc trial. The RGB data was processed as follows:

- A single frame was extracted from the video
- Thresholding was conducted on every frame corresponding to the red color of the marker
- A circle was fit on every marker using the Hough circle transform
- The 2D position of the centers of 5 circles were stored for the every frame
- The MCP, PIP and DIP angles were calculated for every frame using the centers of the circles
- The mean and standard deviation were calculated for the finger pose using data from every frame

This analysis does not show the variation in MCP ad-abduction, however, the force measurements from the axes perpendicular to the forcing direction is enough to show the variation in this joint angle. This procedure is also shown in Fig 4.4.

3.8.4 Force and posture validation

This study requires the subjects to maintain a constant pose and a constant fingertip force. Hence, it was ensured that the force and pose data from the stiffness trials respected the error bounds as follows:

- The total percentage deviation in force was $< 15\%$
- The maximum variation in joint angles was $< 15^{\circ}$

The subject data sets abiding by these error bounds were used in the further processing to stand by the assumptions set down in this study.

3.8.4.1 Principal component analysis

A principal component analysis was done on the processed sEMG data from each of the stiffness trials. The contribution of the each of the 7 components was calculated as a percentage of the total variance in the data. The principal component analysis will output the directions of variability in the data in descending order of contribution to variability. Hence, a principal component analysis will output the directions of stiffness change on each of the iso-torque manifolds. The first principal component is hence forth regarded as the principal synergy. This is the synergy which explains maximum variance in the data. The contributions of all the components were mapped and compared to test the hypothesis.

3.8.5 Comparison of Principal Components

The degree of alignment between the principal components of the trials were calculated as the square root of the absolute value of the dot product between two principal synergies. Here the synergy for distal 40% MVC is denoted as S_{d40} and comparisons are denoted by a :. The within-subject comparisons are as follows:

- Fixed force magnitude but different direction (eg. $S_{d40} : S_{p40}$)
- Fixed force direction but different magnitude (eg. $S_{d40} : S_{d20}$)

The inter subject mean and standard deviation for the degree of alignment were calculated for the cases mentioned above. This comparison shows how these principal synergies vary with force magnitude and direction. Between-subjects principal synergies compared for different force directions were displayed in a gray scale matrix format. The (i, j) element of the matrix for a force condition compared the principal synergies of the i^{th} and j^{th} subject for that condition. A darker matrix entry implies very similar principal synergies.

In order to compare the degree of alignment, a linear mixed effects model was applied to the degree of alignment with subjects as random effects and the comparison cases as the fixed factor (eg. S_{d0}:S_{d60} is one level). The interactions between factor level means were tested to compare the degree of alignment between subjects. A p-value of 0.05 was used to determine statistically significant difference.

3.8.6 Comparison of force and stiffness synergy

The force synergy is denoted as the muscle activation pattern observed at minimum stiffness during a particular experiment. The index of muscle contraction around a joint (IMCJ) for all joints is calculated and summed as an estimate of the total stiffness of the finger. 200 minimum values of the IMCJ were averaged to get the muscle activation pattern at lowest stiffness. This was denoted as the force synergy and the principal synergy from the principal component analysis was denoted as the stiffness synergy. Both were compared to examine the criterion for the choice of these muscle activation pattern.

3.8.7 Stiffness Range

The range of stiffness achieved was calculated as the difference of activation of minimum and maximum IMCJ for the finger. This was normalized to the maximum range to get relative stiffness range for the index finger.

Chapter 4

Results

This chapter contains all the results from the trials explained in the above chapter. Some general observations about the experiments are listed initially. Then individual sections explain the results from each data processing methods.

4.1 General Observations

The subjects reported that they found it easier to co-contract their index finger muscles in trials conducted at lower and distal forces as compared to those at higher and palmar forces respectively. In general, the palmar MVF was higher than that of the distal case. Subjects found it easier to perform the distal force because the distal forces are shared between the flexors and extensors while in the palmar case, only flexors contribute to the majority of the force and stiffness production. Hence, the flexors shared majority of the fingertip load which may have resulted in the difficulty.

4.1.1 Stiffness trials

Figures 4.1 and 4.2 shows the set of accepted data from a stiffness trial for one subject. The 3 peaks in the sEMG data from the muscles are due to the stiffness changes that the subject performed. It is evident from the data that the difference between minimum and maximum stiffness attempted by the subjects decreases as the magnitude of the force increases for the same force direction. The sEMG data in 0% MVF trial goes from 0 muscle activation to a certain maximum. This is because at 0N force the index finger is at complete rest. This confirms the work by others in the literature that the range of achievable stiffness is reduced as the force increases. This has to do with maximum forces that each of the 7 muscles can generate to maintain the fingertip force. At maximal force, the set of achievable force-stiffness is just one point in muscle activation. Note that there is no difference between the 2 0% MVF cases.

The force data from 3 axes of the force sensor during a stiffness experiment is shown in Fig 4.3. The force is exerted on the z axis is fairly constant for the duration of the trials. The forces measured on the other axis are also close to 0N. This is a validation of the assumption that the forces are maintained during the trials.

The angles are calculated from the vision data are shown in Fig 4.4. The circles are found using the circle Hough Transform. The line vectors are calculated to find the angle between them and hence get the finger pose. The data from the trials for which the pose and the force was maintained agree

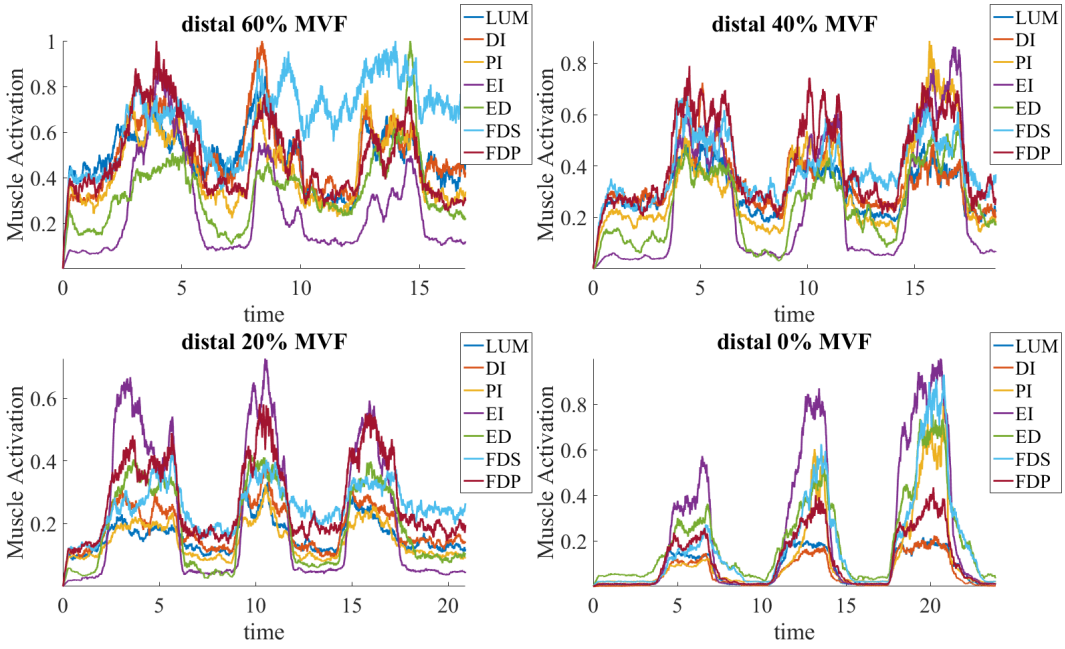

Figure 4.1: sEMG data from stiffness trials with force in distal direction.

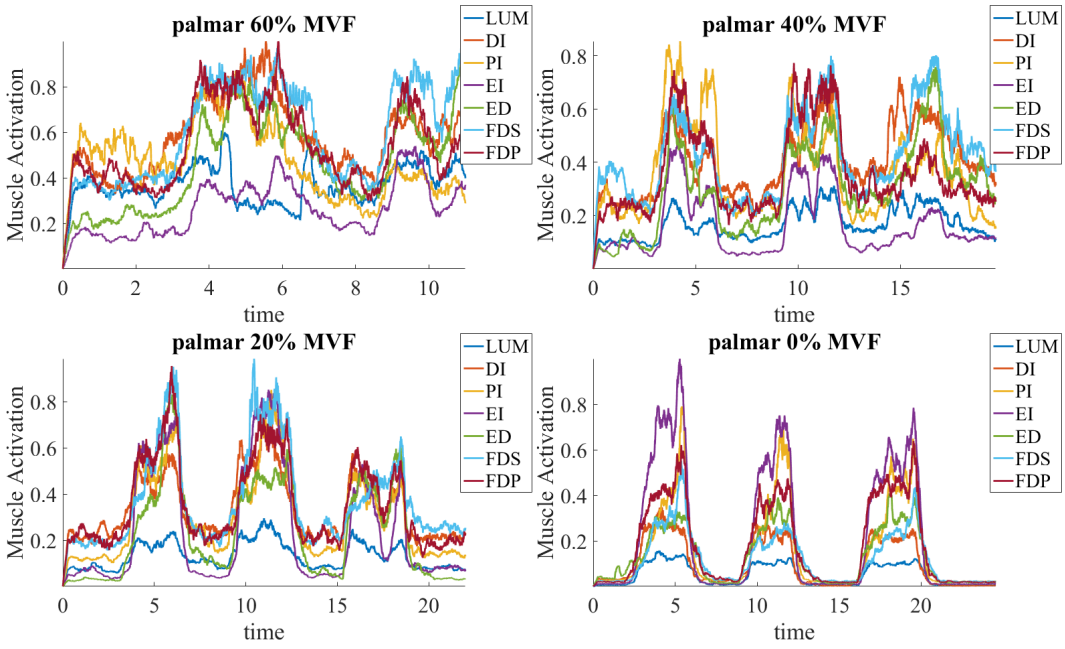

Figure 4.2: sEMG data from stiffness trials with force in palmar direction.

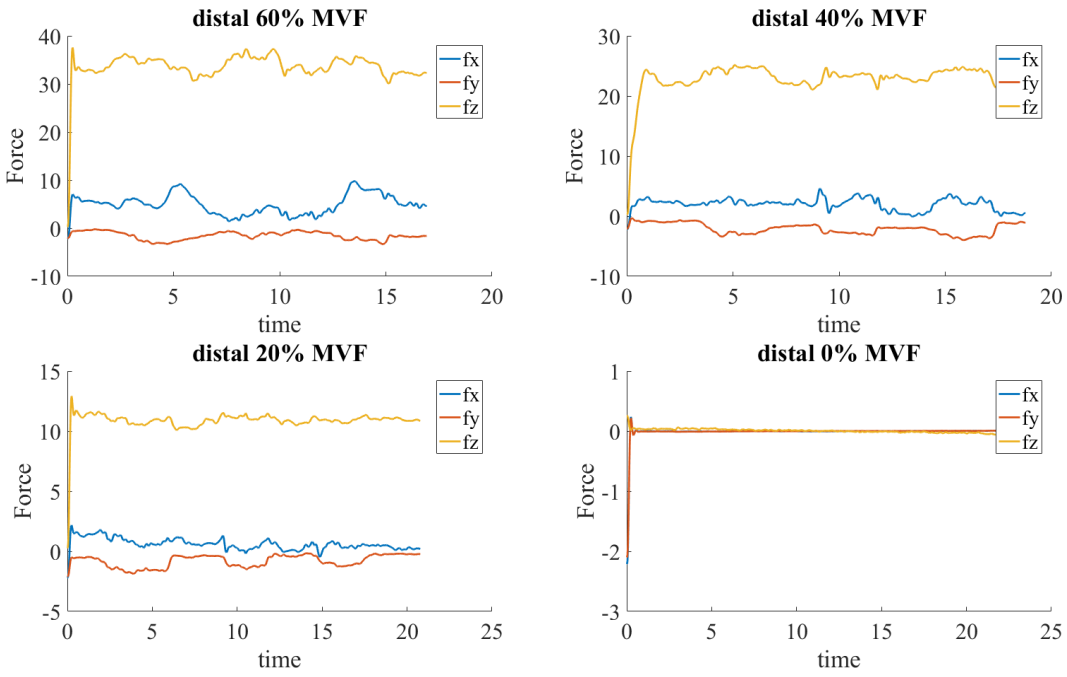

Figure 4.3: Force data from d60,d40,d20 and d0 trials

with the iso-torque assumption. This means that for the entirety of a trial, the muscle activations lie on the iso-torque manifold. The radii of the circles vary throughout the frames but the centers of the circles are used to calculate the vectors and thereafter the angles.

Fig 4.6 shows representative principal synergies for two different force conditions. The muscle activations in the principal synergies were found to be positive for all the muscles. This implies that in order to increase the stiffness of the index finger, the muscle activations of all the muscles were increased.

4.1.2 Principal Component Scores

The average contribution of all the principle components across all subjects (% Mean $\pm$ S.D.) for each of the 8 force conditions is shown (Fig 4.7 and 4.8). The contribution with the standard deviation for the principle synergies for 8 forcing directions from accepted trials of all subjects. The contribution of the principal component reduces with increase in force magnitude. This plot suggests that the contribution is higher and the standard deviation is lower for the distal case. Another observation that can be made here is that the contribution of the principal component to the variance sees a decreasing trend with increasing force. Also, the standard deviation for case of forces in the distal direction are less than those in the palmar direction. The highest contribution were seen at lower force conditions with mean value of around 90%. This value decreases with increasing force to a mean value of around $68 - 70\%$ at 60% MVF condition. Also, in general, the standard deviation

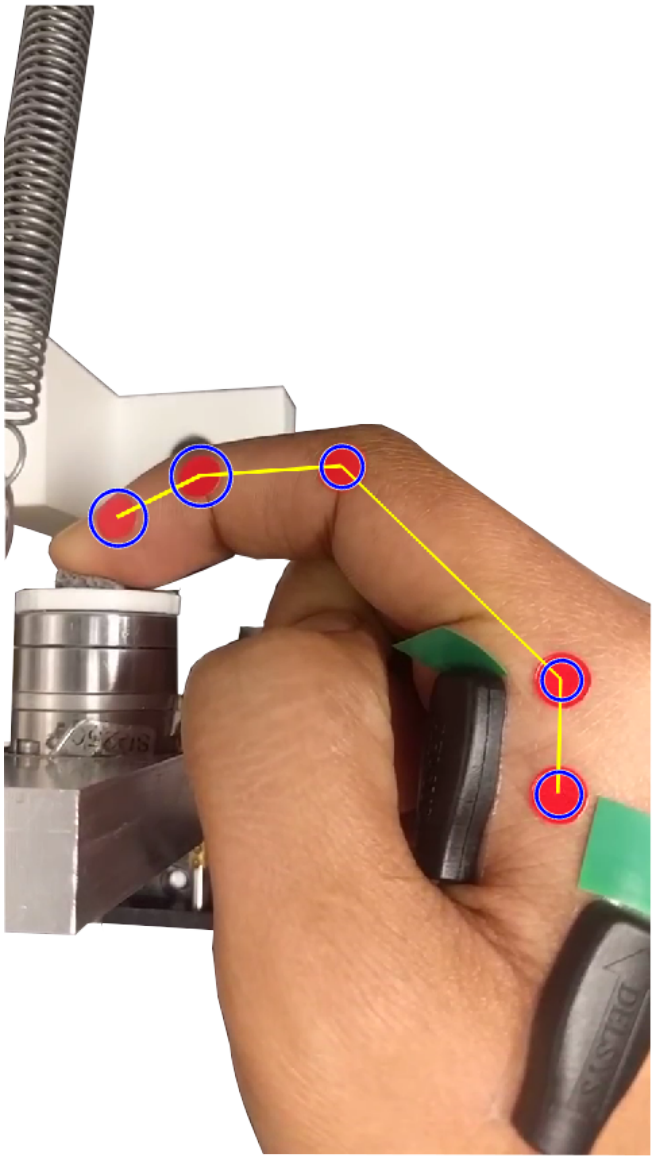

Figure 4.4: Vision data from a trial.

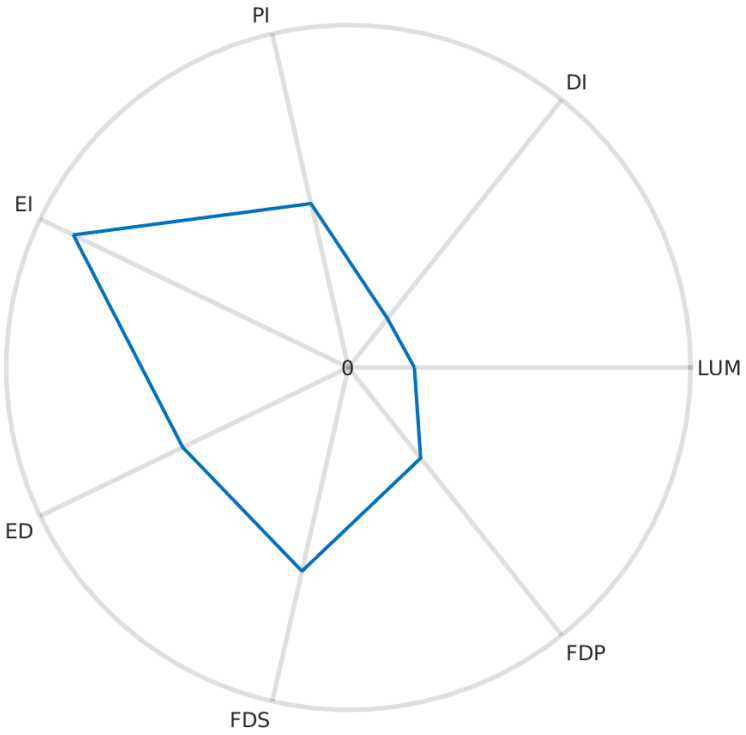

Figure 4.5: S_{d0}

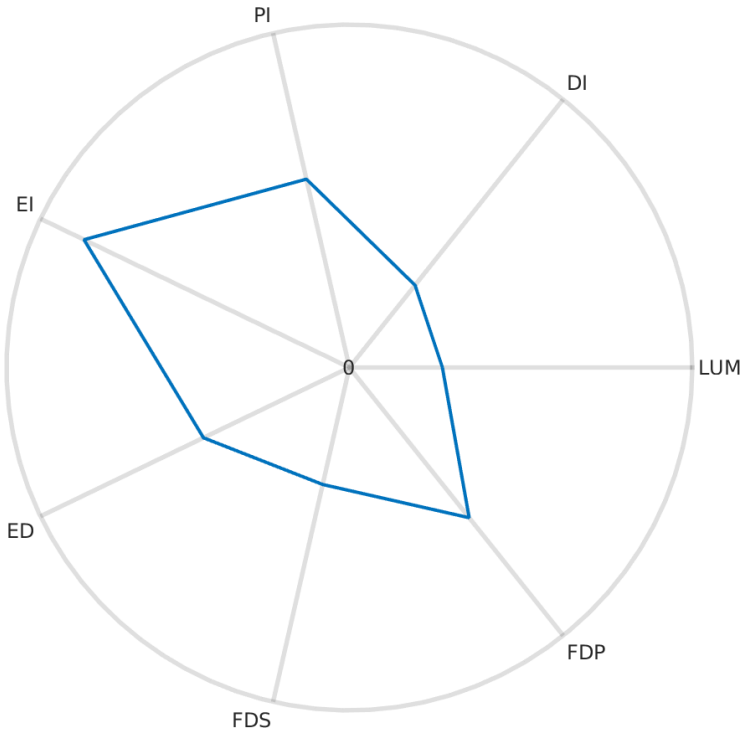

Figure 4.6: S_{d40}

Table 4.1: Average degree of alignment between different force magnitudes (mean ± S.D.).

Comparison	Degree of alignment (mean ± S.D.)
S_{d0}:S_{d20}	0.9311 ± 0.0828
S_{d0}:S_{d40}	0.8984 ± 0.1165
S_{d0}:S_{d60}	0.9045 ± 0.0796
S_{d20}:S_{d40}	0.9582 ± 0.0621
S_{d20}:S_{d60}	0.8985 ± 0.1251
S_{d40}:S_{d60}	0.9112 ± 0.1393

in the contribution is higher at higher forces. The contribution of the second principal component also increases with force magnitude but the mean stays below approximately 15% in all cases. The contribution of all other conmponents is less than 7% for all cases.

4.1.3 Comparison of the principal synergies

Tables 4.1 and 4.2 show the within-subject comparison of principal synergies. Each value is the average degree of alignment of the principal synergies with their respective standard deviation. (Fig 4.9, 4.10 and 4.11) shows the between-subjects comparison of the principal synergies for the same force direction. A darker block corresponds to the principal synergy of the corresponding row and column subjects to be very similar.

4.1.4 Comparison of force and stiffness synergy

Fig 4.12 and 4.13 shows the comparison of force and stiffness synergies for both distal and palmar case.

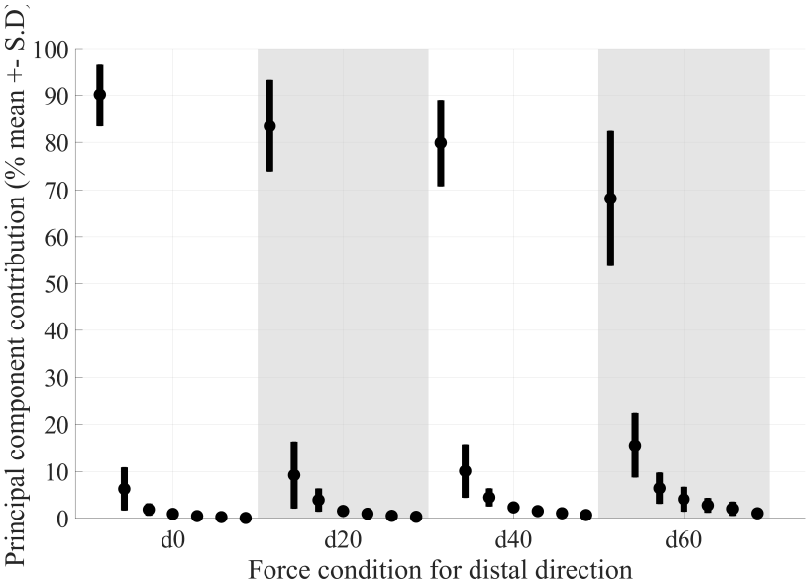

Figure 4.7: Average contribution of each component from the PCA to the total stiffness variation for distal for direction.

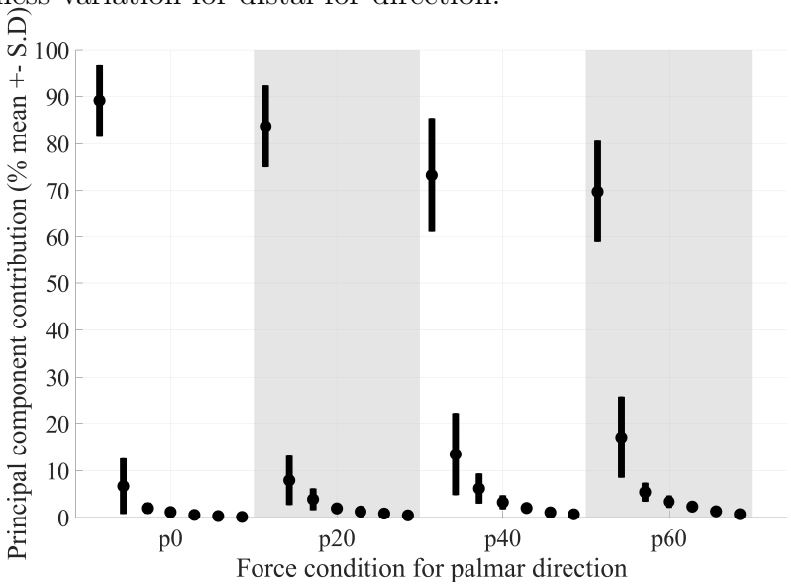

Figure 4.8: Average contribution of each component from the PCA to the total stiffness variation for palmar for direction.

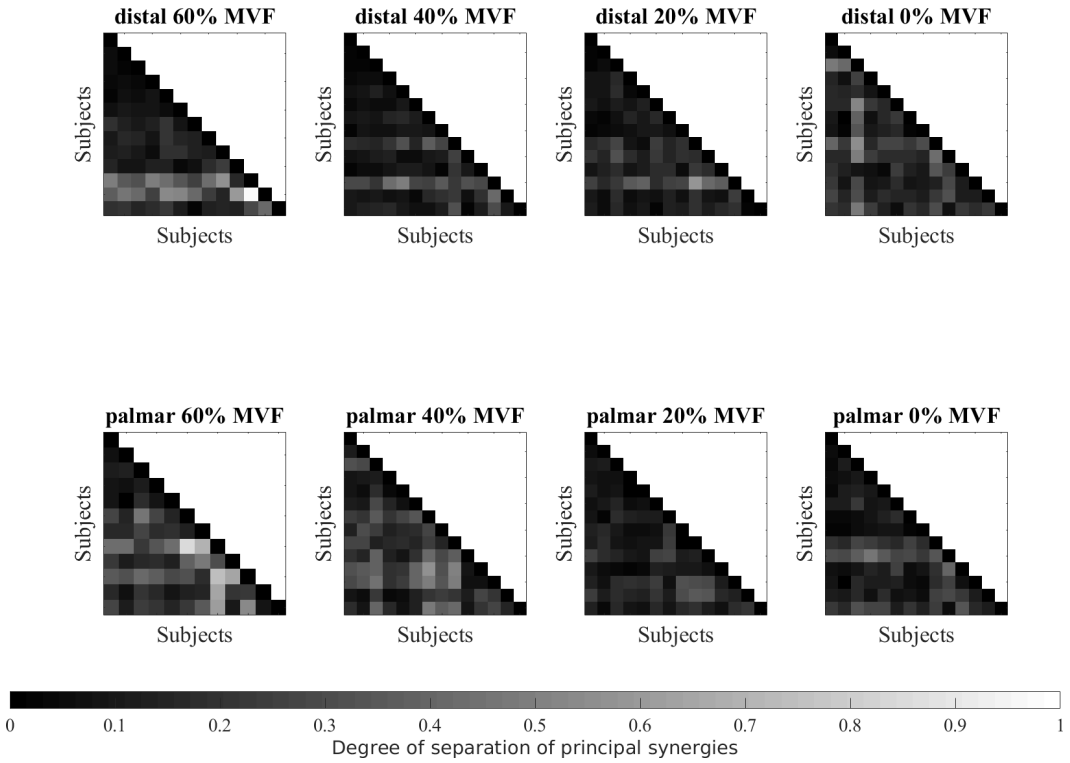

Figure 4.9: Between-subjects comparison of principal synergies for the same force condition.

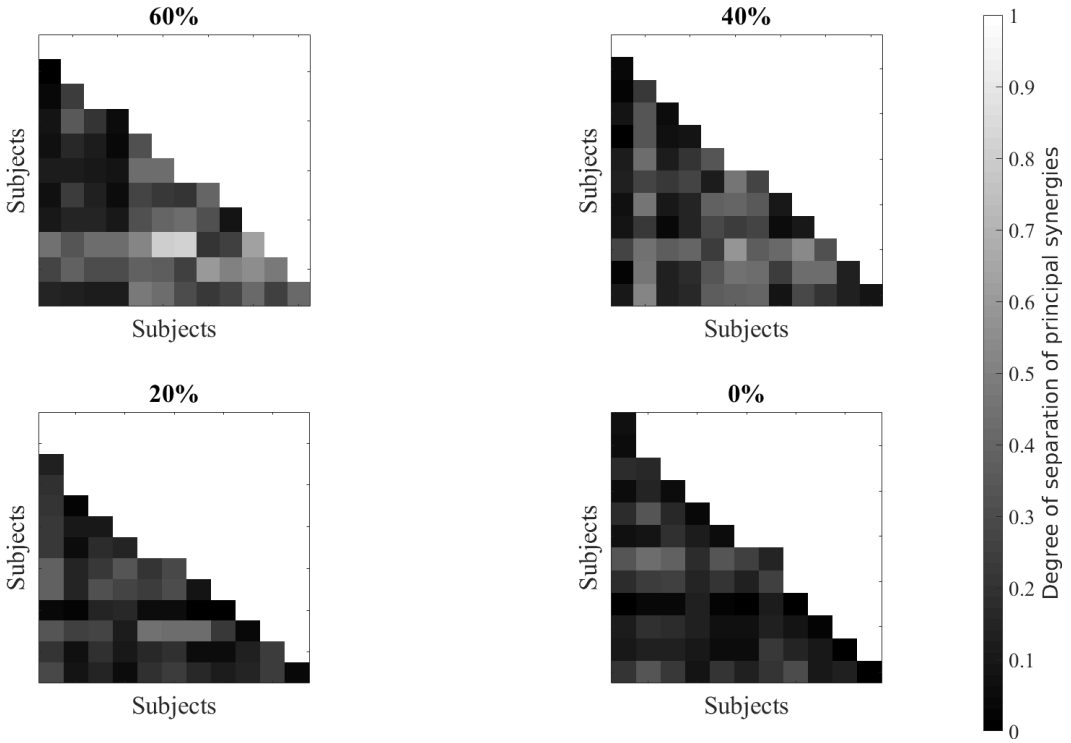

Figure 4.10: Between-subjects comparison of principal synergies for the same force magnitude and different direction.

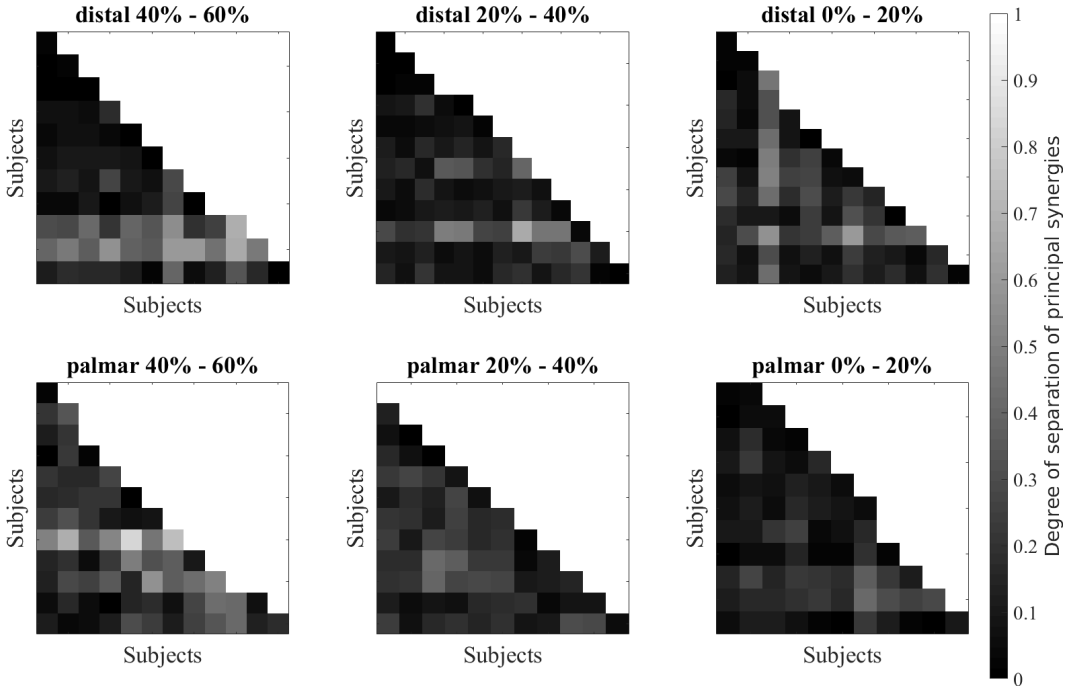

Figure 4.11: Between-subjects comparison of principal synergies for the same force direction and different magnitude.

Table 4.2: Average degree of alignment between different force magnitudes (mean ± S.D.).

Comparison	Degree of alignment (mean ± S.D.)
S_{p0}:S_{p20}	0.9330 ± 0.0541
S_{p0}:S_{p40}	0.9120 ± 0.0481
S_{p0}:S_{p60}	0.8740 ± 0.0757
S_{p20}:S_{p40}	0.9619 ± 0.0308
S_{p20}:S_{p60}	0.9286 ± 0.0563
S_{p40}:S_{p60}	0.8914 ± 0.1473

Table 4.3: Degree of alignment between force conditions of same magnitude but different direction (mean ± S.D.).

Comparison	Degree of alignment (mean ± S.D.)
S_{d0}:S_{p0}	0.9622 ± 0.0283
S_{d20}:S_{p20}	0.9296 ± 0.0462
S_{d40}:S_{p40}	0.9120 ± 0.0600
S_{d60}:S_{p60}	0.8415 ± 0.1302

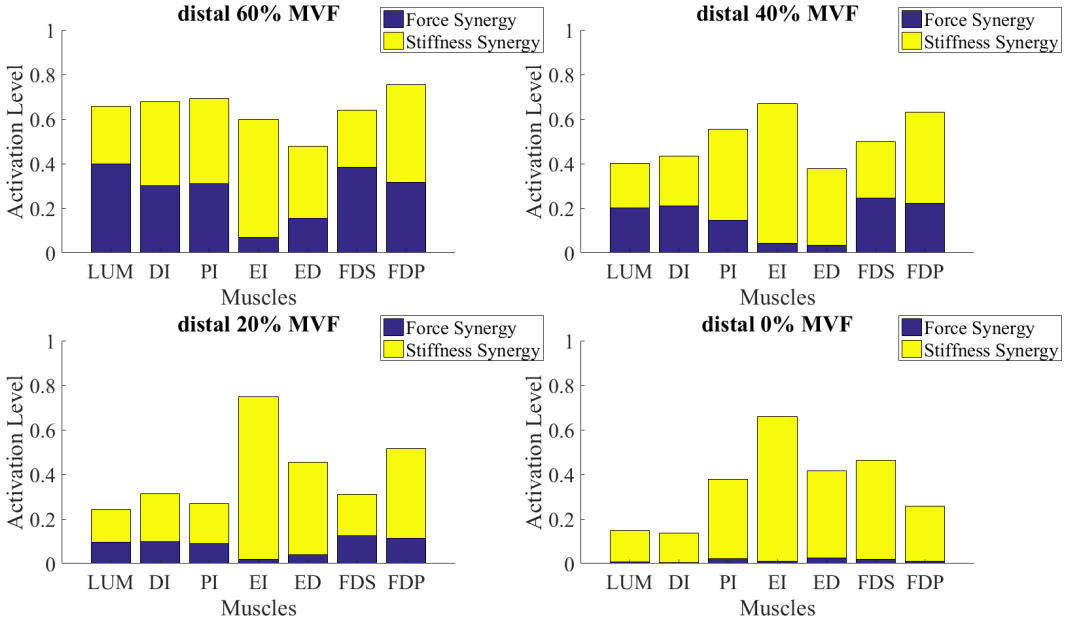

Figure 4.12: Comparison of force and stiffness synergy for distal trials

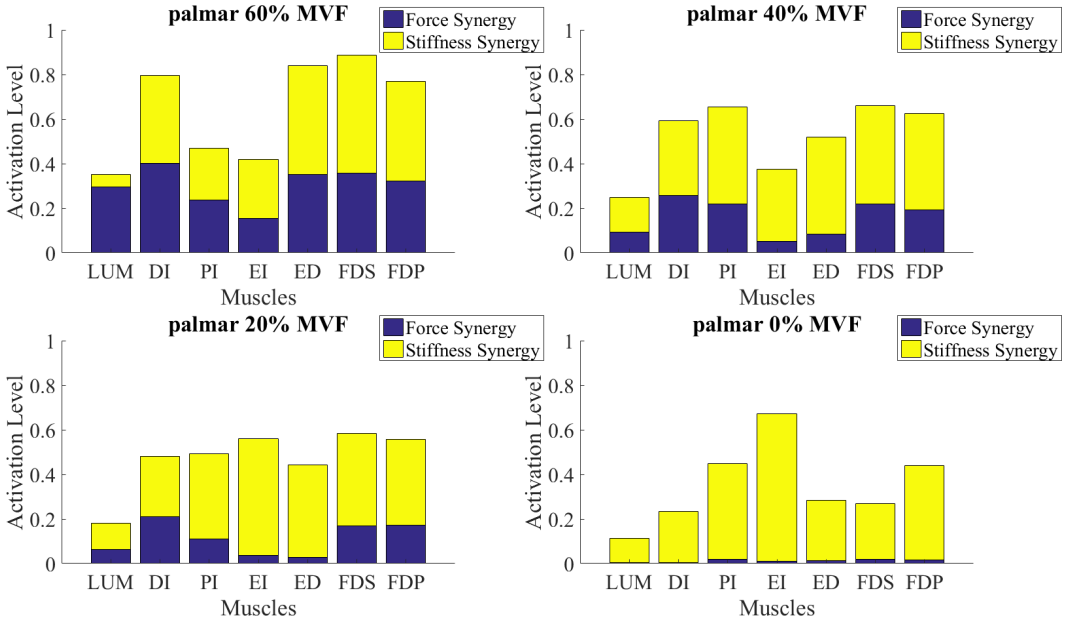

Figure 4.13: Comparison of force and stiffness synergy for palmar trials

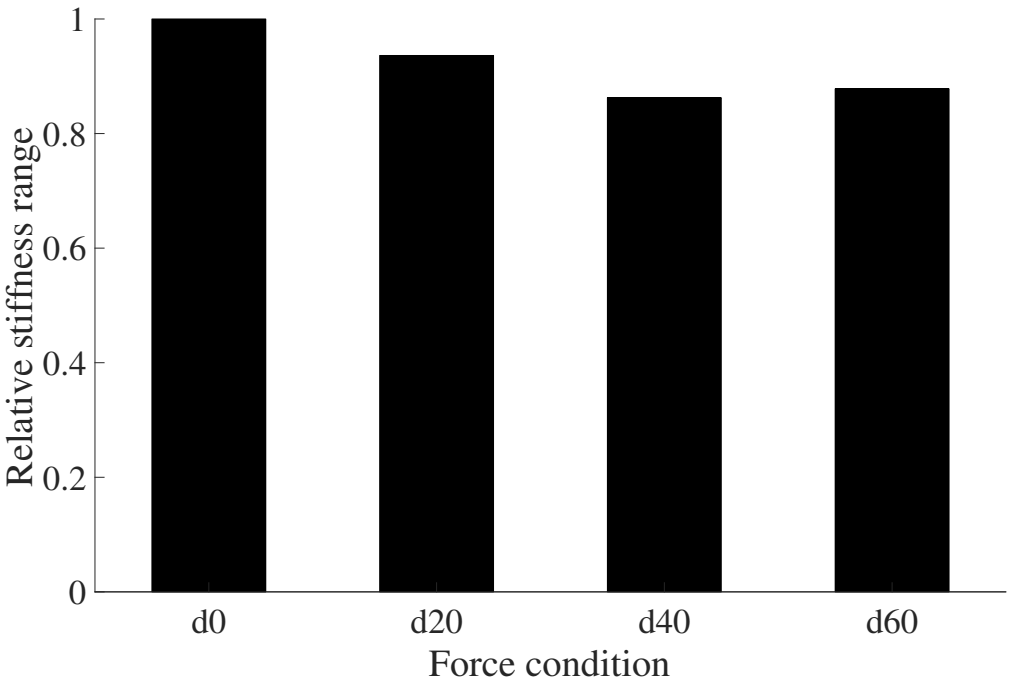

Figure 4.14: The mean relative stiffness range for the distal case.

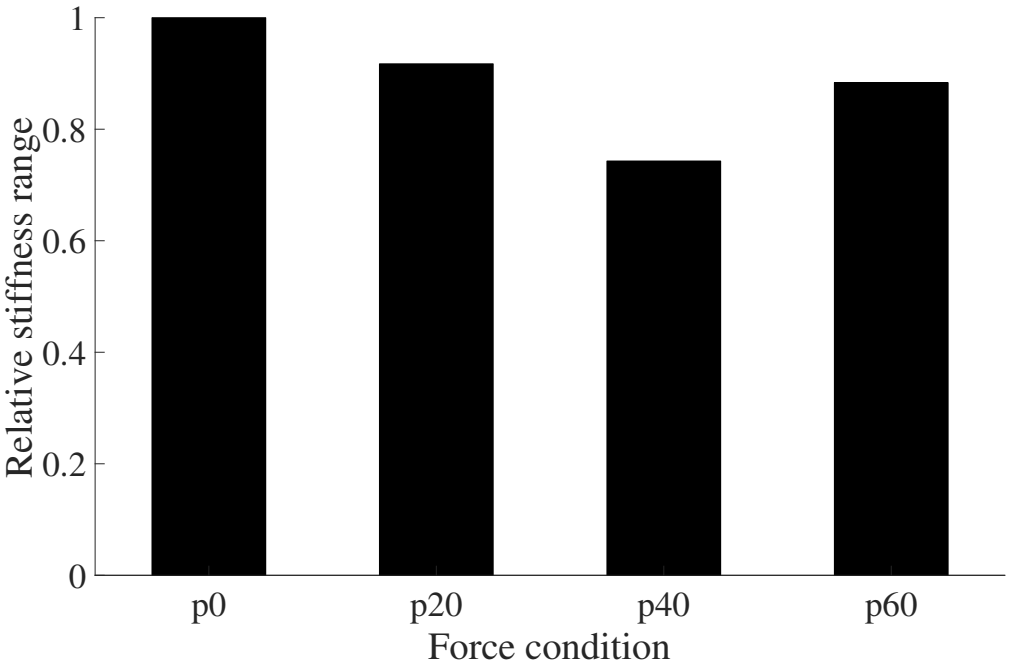

Figure 4.15: The mean relative stiffness range for the palmar case.

Chapter 5

Discussion

This work investigates how humans control their index finger stiffness while exerting a constant fingertip force in isometric conditions. In this study, the requirement of constant fingertip force and pose was simplified to a requirement of fixing finger pose so that the subjects find it easier to perform the experiments and a reliable data set can be obtained. Our hypothesis that a single muscle synergy is responsible for modulating stiffness was confirmed and this muscle synergy corresponds to the nominal muscle activation required to maintain a constant fingertip force and fixed finger pose. We also analyzed the muscle synergy to find structure and extract strategies for neuromuscular control of stiffness. We discuss insights about the choice of these synergies and their relation to fingertip force below.

5.0.5 Experiment Data

Fig 4.1 and 4.2 shows that at lower forces, the subjects are able to co-contract their muscles more than they can at higher forces. The results from [35] supports these observations. Fig 4.3 shows that the errors in the forces maintained by the subjects are less ($< 15\%$ S.D) and hence validates our assumption. This partially validates the variation in finger pose since changing

the finger pose may results in variations in forces. However, the subjects can change their pose in such a way that the fingertip force is maintained. This is validated by the analysis of the vision data. The data that did not comply with the pose requirements was not included in the analysis. The subjects also reported that the palmar cases were more difficult to perform. This is explained by the fact that in order to achieve palmar forces.

5.0.6 Stiffness synergy

The contribution of first principal component for all the force conditions is about five times higher than that of all others (Fig. 4.7 and 4.8). This means that the CNS effectively scales a single muscle synergy in order to modulate the index finger stiffness. The muscles are activated in a particular way to achieve stiffness modulation. A statistical analysis of the stiffness synergies contribution revealed that their contribution is lower at higher forces.

Variation of stiffness synergy with force conditions across subjects shows that the stiffness synergy is different at higher forces (Table 4.1 and 4.2). The p-values and degree of alignment show that the degree of alignment for comparisons made with stiffness synergies at higher forces do not agree with those made at lower forces. This trend is also observed in the comparison of relative stiffness range achieved by the subjects (Fig. 4.14 and 4.15). This indicates a difference in the criterion chosen for stiffness modulation at higher forces. A higher contribution of the second principal component at $d60$ and $p60$ force conditions may be associated with this change.

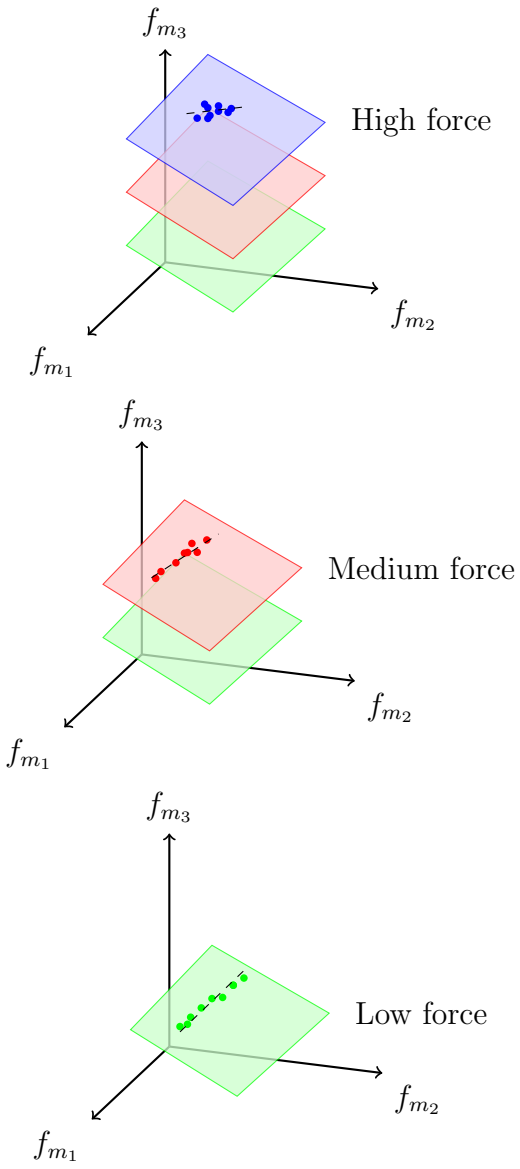

Figure 5.1: This figure shows the visualization of stiffness synergies at different force magnitudes. The planes represent the iso-torque plan in muscle activation space for every force. (a),(b) and (c) show that as the force magnitude increases, the range of stiffness reduces and the principal component may become susceptible to variations.

5.0.7 Neuromuscular criteria for motor control

From the perspective of motor control, researchers have introduced opposing theories to explain neuromuscular strategies. On one side, a set of theories posit that nature follows a sense of optimality for resolving redundancy. Previous studies have focussed on optimal control of redundant musculoskeletal system with a cost function which minimizes biological criterion like energy, fatigue and stress [36]. On the other hand, a set of theories present the idea of minimum variability in task irrelevant parameters while making ensuring task relevant goals are achieved. Theories including uncontrolled manifold hypothesis, threshold control theory and minimum intervention principle [20, 26, 28, 38, 41, 42] have been developed in the past which fall in this catagory.

In the context of stiffness control, it was hypothesized that the CNS sometimes chooses between minimal energy solution and a faster and simpler solution to achieve force-stiffness conditions [4]. This idea was used to explain the two different muscle synergies found in the above conditions. However, it was unclear what criterion the CNS chooses to switch between the two stretegies. Our results may shed light on this topic. Our data shows that at low and medium values of the end point forces the modulation of stiffness is achieved by simply scaling the muscle synergy achieved at nominal stiffness values. But under the conditions of high end-point force values, this scaling strategy does not seem to work. So, the CNS seems to recruit additional synergies to modulate stiffness. This change in strategy could be because at

higher forces, it may be critical and advantageous to minimize effort. While our data illustrates a switch in neuromuscular strategy at higher forces, the underlying mechanism behind this switching is still unclear.

The limitation of our work is that we mainly focus on the physiological aspects of stiffness control which explain the neuromuscular strategies used to control stiffness. Previous studies which have focussed on the behavioral measures of stiffness, also explain the output of these strategies which is the actual stiffness ellipse achieved in limbs. Studies conducted with both the measures will help understand the exact stiffness ellipse at given muscle activations. Future work in this direction may prove fruitful in examining end-to-end control of stiffness and muscle forces. Another limitation of our work is in the choice of surface electromyography sensors over intramuscular EMG sensors for measuring muscle activity. Although intramuscular EMG sensors are known to provide precise and extra information about muscle activity, sEMG sensors measure the muscle activation over a larger area of the muscle belly.

5.1 Conclusion and Future Work

This work investigates the muscle activation patterns for isometric voluntary stiffness modulation at constant index fingertip for and finger pose. A unique experimental platform was developed to fix the force and pose while the subjects were asked to modulate their whole finger stiffness. Experimental results revealed that stiffness is modulated by scaling a single muscle synergy ($\tilde{8}$0%-95% contribution). This synergy was found to vary more with the direc-

tion of fingertip force as compared to force magnitude. No conclusive results were obtained for higher forces or when some muscles were close to maximum activation. The force and stiffness synergies were compared for every force direction and were muscle activations seem to have an inverse relation. To the best of our knowledge, this kind of investigation of stiffness control in human index finger has not been done before. Our hope is that this result will further the understanding of redundancy in the index finger.

The ultimate goal of this work is to find a mapping or a criterion to decide the muscle activation patterns given the finger pose, fingertip force and the finger stiffness. In order to achieve this, measurement of all the 3 fundamental motor outputs is essential. Knowing the precise neuromuscular control of the index finger will greatly help in making human-like prosthetic limbs which will enable maximum restoration of hand function.

Bibliography

[1] Pedram Afshar. *A neuromuscular framework for motor control*. PhD thesis, Carnegie Mellon University, 2007.

[2] David Amarantini and Luc Martin. A method to combine numerical optimization and emg data for the estimation of joint moments under dynamic conditions. *Journal of biomechanics*, 37(9):1393–1404, 2004.

[3] Kai-Nan An, Y Ueba, EY Chao, WP Cooney, and RL Linscheid. Tendon excursion and moment arm of index finger muscles. *Journal of biomechanics*, 16(6):419–425, 1983.

[4] Ravi Balasubramanian and Yoky Matsuoka. Biological stiffness control strategies for the anatomically correct testbed (act) hand. In *Robotics and Automation, 2008. ICRA 2008. IEEE International Conference on*, pages 737–742. IEEE, 2008.

[5] Ravi Balasubramanian and Yoky Matsuoka. The role of small redundant actuators in precise manipulation. In *Robotics and Automation, 2009. ICRA'09. IEEE International Conference on*, pages 4409–4415. IEEE, 2009.

[6] Nikolaj A Bernstein. The co-ordination and regulation of movements. 1967.

[7] Paul W Brand and Anne Hollister. *Clinical mechanics of the hand*. Mosby Incorporated, 1999.

[8] N Brook, J Mizrahi, M Shoham, and J Dayan. A biomechanical model of index finger dynamics. *Medical engineering & physics*, 17(1):54–63, 1995.

[9] Stephen HM Brown and Stuart M McGill. Muscle force–stiffness characteristics influence joint stability: a spine example. *Clinical Biomechanics*, 20(9):917–922, 2005.

[10] V. Bundhoo and E. J. Park. Design of an artificial muscle actuated finger towards biomimetic prosthetic hands. In *ICAR '05. Proceedings., 12th International Conference on Advanced Robotics, 2005.*, pages 368–375, July 2005.

[11] Charles G Burgar, Francisco J Valero-Cuevas, and Vincent R Hentz. Fine-wire electromyographic recording during force generation: Application to index finger kinesiologic studies. *American journal of physical medicine & rehabilitation*, 76(6):494–501, 1997.

[12] EYS Chao, KN An, WP Cooney, and RL Linscheid. Normative model of human hand. *Biomechanics of the Hand: A Basic Research Study. World Scientific Publishing Co. Pte. Ltd., Singapore*, 1989.

[13] Jacek Cholewicki and Stuart M McGill. Emg assisted optimization: a

hybrid approach for estimating muscle forces in an indeterminate biomechanical model. *Journal of biomechanics*, 27(10):1287–1289, 1994.

[14] CS Cook and M JN McDonagh. Measurement of muscle and tendon stiffness in man. *European journal of applied physiology and occupational physiology*, 72(4):380–382, 1996.

[15] Carlo J De Luca, L Donald Gilmore, Mikhail Kuznetsov, and Serge H Roy. Filtering the surface EMG signal: Movement artifact and baseline noise contamination. *Journal of biomechanics*, 43(8):1573–1579, may 2010.

[16] Ashish D. Deshpande, Ravi Balasubramanian, Jonathan Ko, and Yoky Matsuoka. Acquiring variable moment arms for index finger using a robotic testbed. *Biomedical Engineering, IEEE Transactions on*, 57(8):2034–2044, 2010.

[17] Ahmet Erdemir, Scott McLean, Walter Herzog, and Antonie J van den Bogert. Model-based estimation of muscle forces exerted during movements. *Clinical biomechanics*, 22(2):131–154, 2007.

[18] Anatol G Feldman. Functional tuning of the nervous system with control of movement or maintenance of a steady posture. ii. controllable parameters of the muscle. *Biophysics*, 11:565–578, 1966.

[19] Anatol G Feldman. Once more on the equilibrium-point hypothesis (λ model) for motor control. *Journal of motor behavior*, 18(1):17–54, 1986.

[20] Anatol G. Feldman and Mindy F. Levin. *The Equilibrium-Point Hypothesis – Past, Present and Future*, pages 699–726. Springer US, Boston, MA, 2009.

[21] NK Fowler, Alexander C Nicol, B Condon, and D Hadley. Method of determination of three dimensional index finger moment arms and tendon lines of action using high resolution mri scans. *Journal of biomechanics*, 34(6):791–797, 2001.

[22] Denis Gagnon, Christian Larivière, and Patrick Loisel. Comparative ability of emg, optimization, and hybrid modelling approaches to predict trunk muscle forces and lumbar spine loading during dynamic sagittal plane lifting. *Clinical Biomechanics*, 16(5):359–372, 2001.

[23] Joseph Hamill and Kathleen M Knutzen. *Biomechanical basis of human movement*. Lippincott Williams & Wilkins, 2006.

[24] Joshua M Inouye and Francisco J Valero-Cuevas. Muscle synergies heavily influence the neural control of arm endpoint stiffness and energy consumption. *PLoS Comput Biol*, 12(2):e1004737, 2016.

[25] Kevin G. Keenan, Veronica J. Santos, Madhusudhan Venkadesan, and Francisco J. Valero-Cuevas. Maximal voluntary fingertip force production is not limited by movement speed in combined motion and force tasks. *Journal of Neuroscience*, 29(27):8784–8789, 2009.

[26] Mark L Latash. Motor synergies and the equilibrium-point hypothesis. *Motor control*, 14(3):294–322, 2010.

[27] Sang Wook Lee, Hua Chen, Joseph D. Towles, and Derek G. Kamper. Estimation of the effective static moment arms of the tendons in the index finger extensor mechanism. *Journal of Biomechanics*, 41(7):1567 – 1573, 2008.

[28] Dan Liu and Emanuel Todorov. Evidence for the flexible sensorimotor strategies predicted by optimal feedback control. *Journal of Neuroscience*, 27(35):9354–9368, 2007.

[29] Gerald E Loeb. Optimal isnt good enough. *Biological cybernetics*, 106(11-12):757–765, 2012.

[30] Silvestro Micera, Jacopo Carpaneto, and Stanisa Raspopovic. Control of hand prostheses using peripheral information. *IEEE reviews in biomedical engineering*, 3:48–68, jan 2010.

[31] Theodore E Milner and David W Franklin. Characterization of multijoint finger stiffness: dependence on finger posture and force direction. *IEEE Transactions on Biomedical Engineering*, 45(11):1363–1375, 1998.

[32] Mojtaba Mirakhorlo, Judith MA Visser, BAAX Goislard de Monsabert, FCT Van der Helm, H Maas, and HEJ Veeger. Anatomical parameters for musculoskeletal modeling of the hand and wrist. *International Biomechanics*, 3(1):40–49, 2016.

[33] Frank Henry Netter, Sharon Colacino, et al. *Atlas of human anatomy*, volume 11. Ciba-Geigy Summit, NJ, 1989.

[34] Behnoosh Parsa, Satyajit Ambike, Alexander Terekhov, Vladimir M Zatsiorsky, and Mark L Latash. Analytical inverse optimization in two-hand prehensile tasks. *Journal of motor behavior*, 48(5):424–434, 2016.

[35] Eric J Perreault, Robert F Kirsch, and Patrick E Crago. Voluntary control of static endpoint stiffness during force regulation tasks. *Journal of neurophysiology*, 87(6):2808–2816, 2002.

[36] Boris I Prilutsky and Vladimir M Zatsiorsky. Optimization-based models of muscle coordination. *Exercise and sport sciences reviews*, 30(1):32, 2002.

[37] X Sancho-Bru, FJ Valero-Cuevas, A Pérez-González, DJ Giurintano, M Vergara-Monedero, and FT Sánchez-Marın. Modeling the metacarpophalangeal joint in a biomechanical model of the index finger. In *Fifth International symposium on computer methods in Biomechanics and Biomedical Engineering*, 2001.

[38] John P Scholz and Gregor Schöner. The uncontrolled manifold concept: identifying control variables for a functional task. *Experimental brain research*, 126(3):289–306, 1999.

[39] Reza Shadmehr and Michael A Arbib. A mathematical analysis of the force-stiffness characteristics of muscles in control of a single joint system.

Biological cybernetics, 66(6):463–477, 1992.

[40] Evangelos Theodorou, Emanuel Todorov, and Francisco J Valero-Cuevas. Neuromuscular stochastic optimal control of a tendon driven index finger model. In *American Control Conference (ACC), 2011*, pages 348–355. IEEE, 2011.

[41] Emanuel Todorov. Optimality principles in sensorimotor control. *Nature neuroscience*, 7(9):907–915, 2004.

[42] Emanuel Todorov and Michael I Jordan. Optimal feedback control as a theory of motor coordination. *Nature neuroscience*, 5(11):1226–1235, 2002.

[43] F. J. Valero-Cuevas, J. W. Yi, D. Brown, R. V. McNamara, C. Paul, and H. Lipson. The tendon network of the fingers performs anatomical computation at a macroscopic scale. *IEEE Transactions on Biomedical Engineering*, 54(6):1161–1166, June 2007.

[44] Francisco J Valero-Cuevas. Predictive modulation of muscle coordination pattern magnitude scales fingertip force magnitude over the voluntary range. *Journal of Neurophysiology*, 83(3):1469–1479, 2000.

[45] Francisco J Valero-Cuevas. An integrative approach to the biomechanical function and neuromuscular control of the fingers. *Journal of Biomechanics*, 38(4):673–684, 2005.

[46] Francisco J. Valero-Cuevas. *A Mathematical Approach to the Mechanical Capabilities of Limbs and Fingers*, pages 619–633. Springer US, Boston, MA, 2009.

[47] Francisco J. Valero-Cuevas, Joseph D. Towles, and Vincent R. Hentz. Quantification of fingertip force reduction in the forefinger following simulated paralysis of extensor and intrinsic muscles. *Journal of Biomechanics*, 33(12):1601 – 1609, 2000.

[48] Francisco J Valero-Cuevas, Madhusudhan Venkadesan, and Emanuel Todorov. Structured variability of muscle activations supports the minimal intervention principle of motor control. *Journal of Neurophysiology*, 102(1):59–68, 2009.

[49] Francisco J Valero-Cuevas, Felix E Zajac, and Charles G Burgar. Large index-fingertip forces are produced by subject-independent patterns of muscle excitation. *Journal of biomechanics*, 31(8):693–703, 1998.

[50] Madhusudhan Venkadesan and Francisco J. Valero-Cuevas. Neural control of motion-to-force transitions with the fingertip. *Journal of Neuroscience*, 28(6):1366–1373, 2008.

[51] Laurent Vigouroux, Franck Quaine, Annick Labarre-Vila, David Amarantini, and François Moutet. Using emg data to constrain optimization procedure improves finger tendon tension estimations during static fingertip force production. *Journal of biomechanics*, 40(13):2846–2856, 2007.

[52] John Z Wu, Kai-Nan An, Robert G Cutlip, and Ren G Dong. A practical biomechanical model of the index finger simulating the kinematics of the muscle/tendon excursions. *Bio-medical materials and engineering*, 20(2):89–97, 2010.